Supplementary Information

On the Fluorescent, Steric and Electronic Factors Affecting the Detection of Metallic Ions Using an Imidazolyl-Phenolic Derived Fluorescent Probe

Ronaldo B. Orfão Jr., Fabricio de Carvalho, Paula Homem-de-Mello and Fernando H. Bartoloni*

Centro de Ciências Naturais e Humanas, Universidade Federal do ABC, 09210-580 Santo André-SP, Brazil

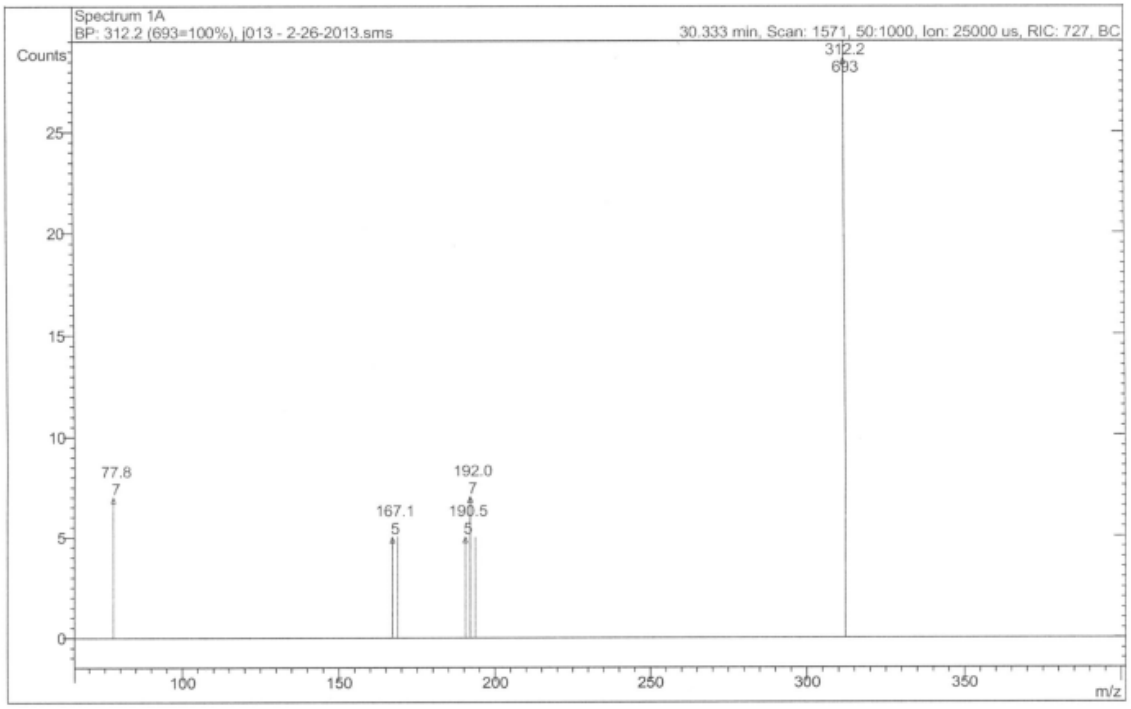

Figure S1. MS spectra of **1**.

*e-mail: fernando.bartoloni@ufabc.edu.br

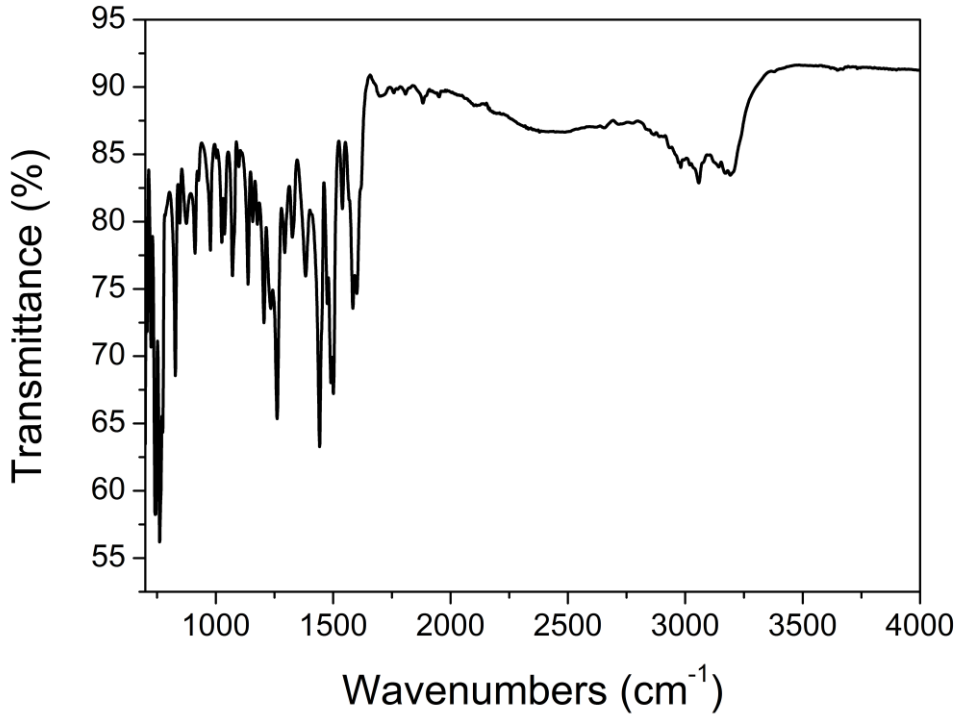

Figure S2. ATR-IR spectra of **1**.

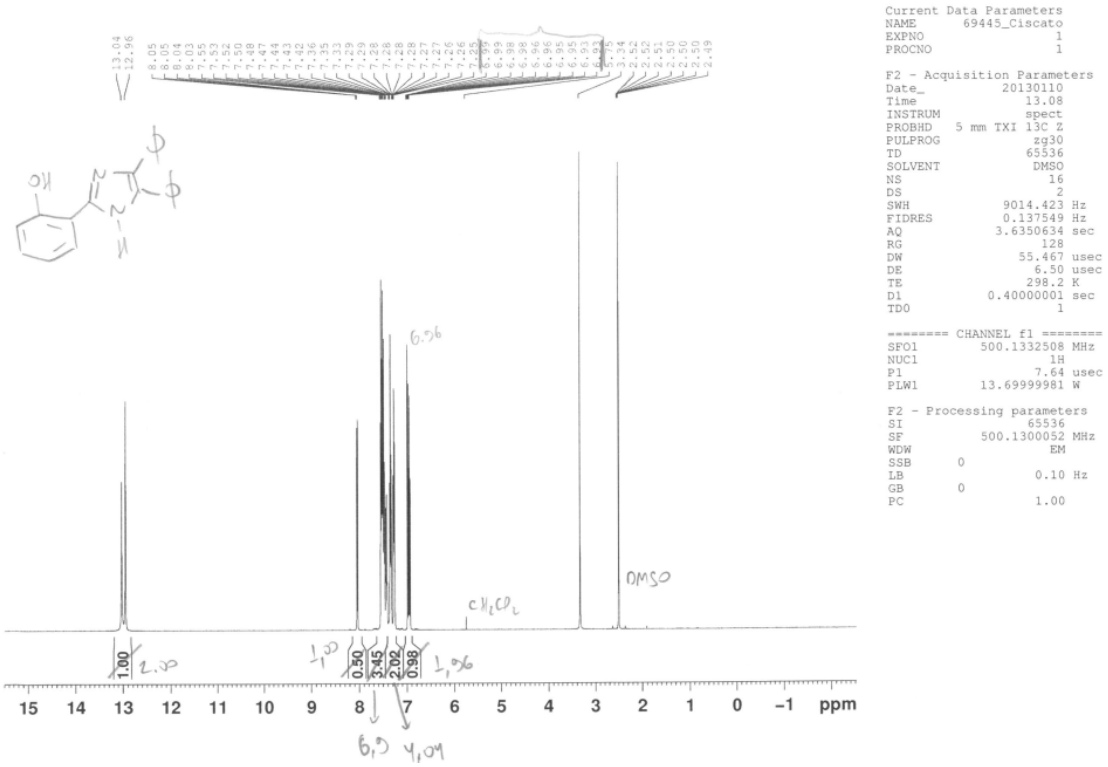

Figure S3. ^{1}H NMR (500 MHz, DMSO-d_6) spectra of **1**.

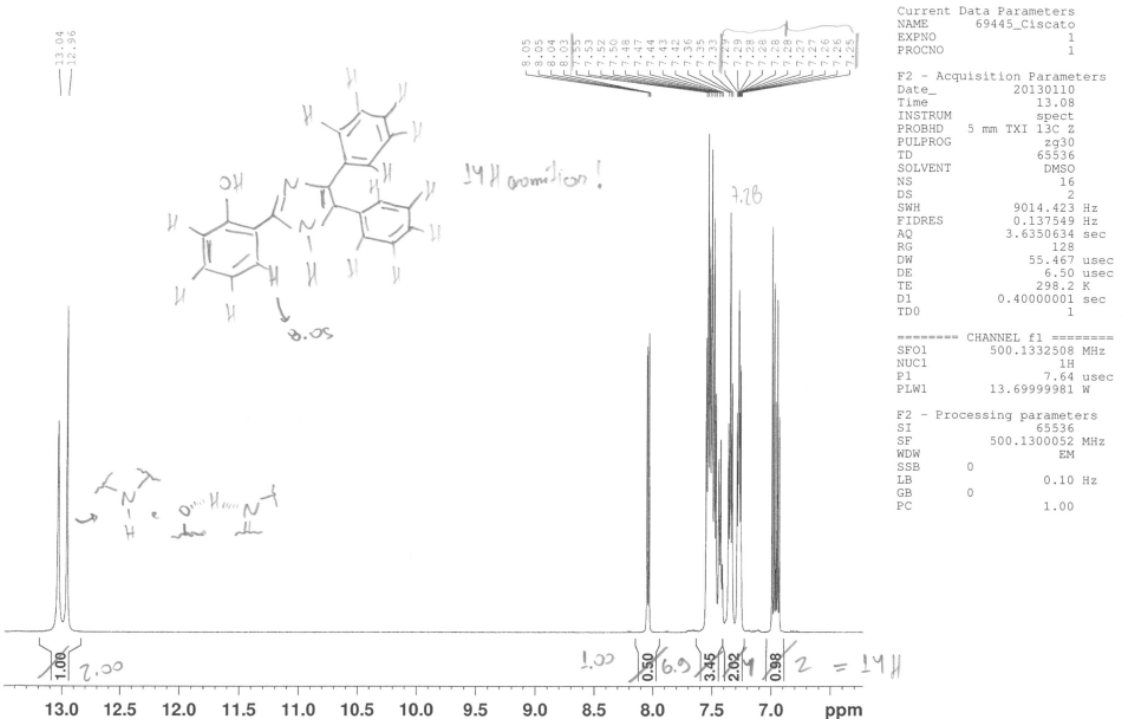


```
Current Data Parameters
NAME         69445_Ciscato
EXPNO                    1
PROCNO                   1

F2 - Acquisition Parameters
Date_             20130110
Time                 13.08
INSTRUM              spect
PROBHD    5 mm TXI 13C Z
PULPROG              zg30
TD                  65536
SOLVENT              DMSO
NS                     16
DS                      2
SWH               9014.423 Hz
FIDRES            0.137549 Hz
AQ                3.6350634 sec
RG                     128
DW                  55.467 usec
DE                    6.50 usec
TE                  298.2 K
D1              0.40000001 sec
TD0                     1

======== CHANNEL f1 ========
SFO1            500.1332508 MHz
NUC1                    1H
P1                    7.64 usec
PLW1           13.69999981 W

F2 - Processing parameters
SI                    65536
SF              500.1300052 MHz
WDW                     EM
SSB          0
LB                    0.10 Hz
GB           0
PC                    1.00
```

Figure S3. [1]H NMR (500 MHz, DMSO-d_6) spectra of **1** (cont.).

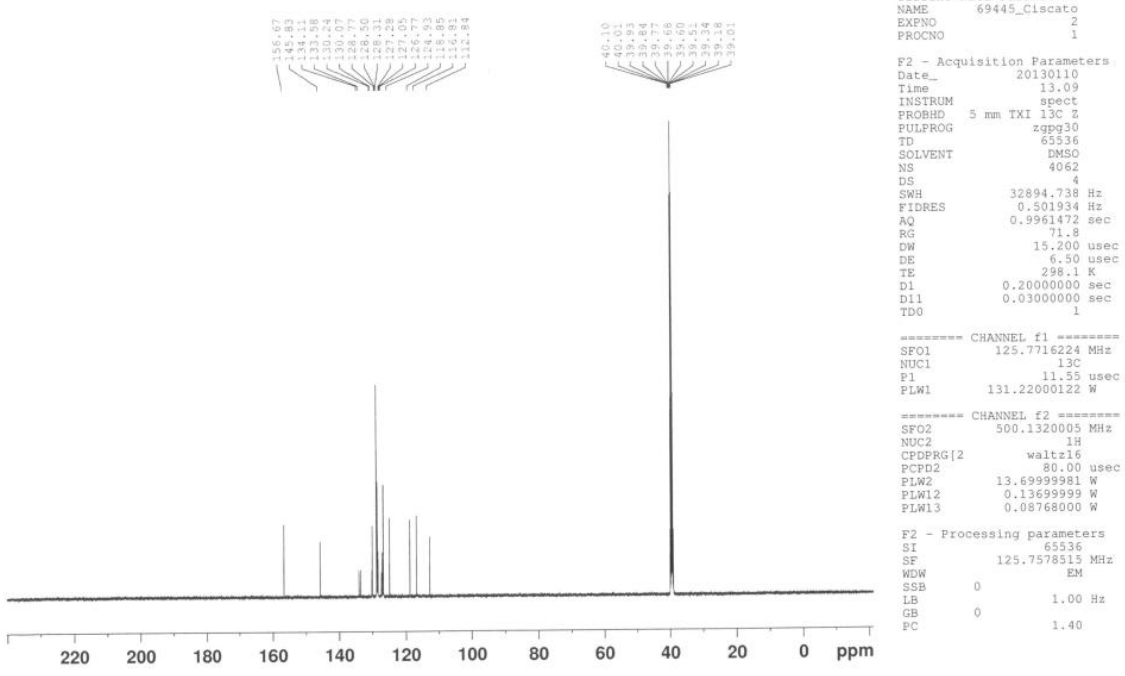


```
Current Data Parameters
NAME         69445_Ciscato
EXPNO                    2
PROCNO                   1

F2 - Acquisition Parameters
Date_             20130110
Time                 13.09
INSTRUM              spect
PROBHD    5 mm TXI 13C Z
PULPROG           zgpg30
TD                  65536
SOLVENT              DMSO
NS                   4062
DS                      4
SWH              32894.738 Hz
FIDRES            0.501934 Hz
AQ                0.9961472 sec
RG                     71.8
DW                  15.200 usec
DE                    6.50 usec
TE                  298.1 K
D1              0.20000000 sec
D11             0.03000000 sec
TD0                     1

======== CHANNEL f1 ========
SFO1           125.7716224 MHz
NUC1                   13C
P1                   11.55 usec
PLW1          131.22000122 W

======== CHANNEL f2 ========
SFO2            500.1320005 MHz
NUC2                    1H
CPDPRG[2          waltz16
PCPD2                80.00 usec
PLW2           13.69999981 W
PLW12           0.13699999 W
PLW13           0.08768000 W

F2 - Processing parameters
SI                    65536
SF             125.7578515 MHz
WDW                     EM
SSB          0
LB                    1.00 Hz
GB           0
PC                    1.40
```

Figure S4. [13]C NMR (125 MHz, DMSO-d_6) spectra of **1**.

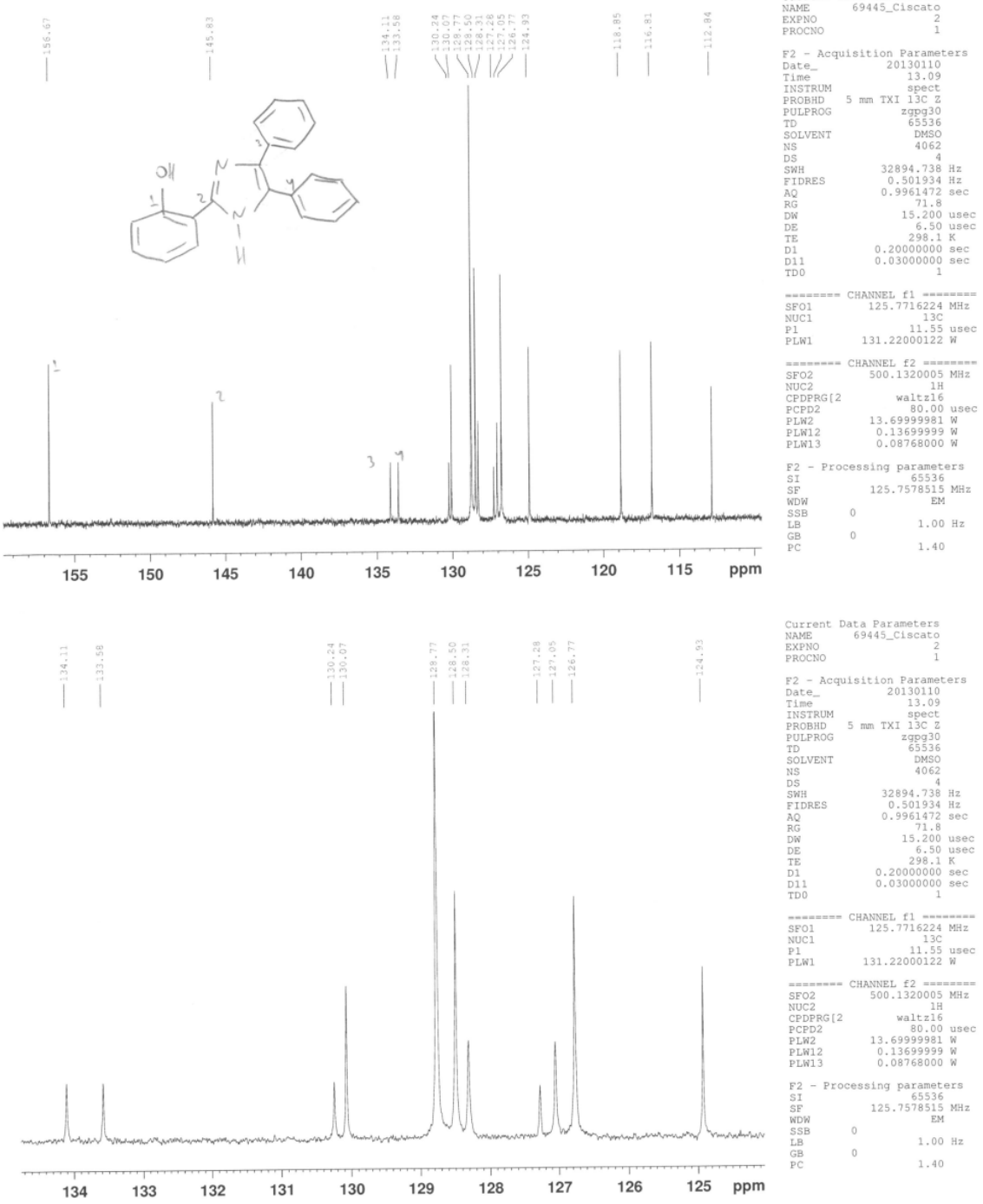

Figure S4. ^{13}C NMR (125 MHz, DMSO-d_6) spectra of **1** (cont.).

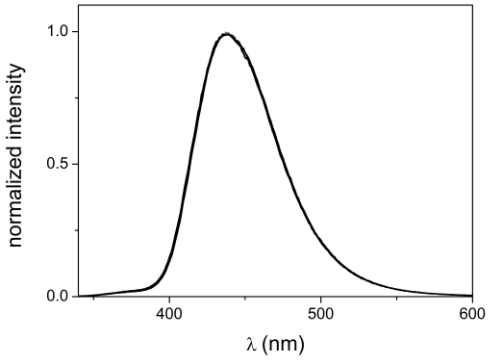

Figure S5. Effect of Ca^{2+} concentration (1.3×10^{-6} to 2.6×10^{-5} mol L^{-1}) on the fluorescence emission profile of **1** in CH_3CN/H_2O (95/5, v/v).

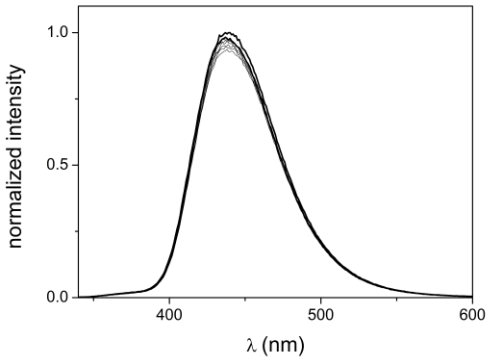

Figure S6. Effect of Co^{2+} concentration (1.3×10^{-6} to 2.5×10^{-5} mol L^{-1}) on the fluorescence emission profile of **1** in CH_3CN/H_2O (95/5, v/v).

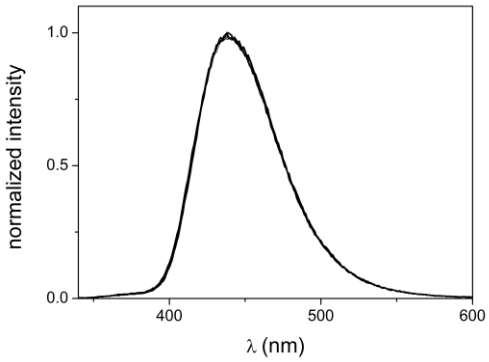

Figure S7. Effect of Ni^{2+} concentration (1.5×10^{-6} to 2.9×10^{-5} mol L^{-1}) on the fluorescence emission profile of **1** in CH_3CN/H_2O (95/5, v/v).

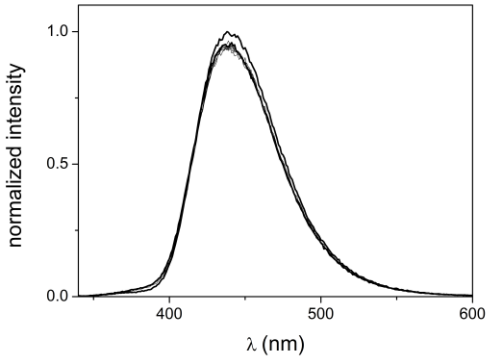

Figure S8. Effect of Zn^{2+} concentration (1.2×10^{-6} to 2.4×10^{-5} mol L^{-1}) on the fluorescence emission profile of **1** in CH_3CN/H_2O (95/5, v/v).

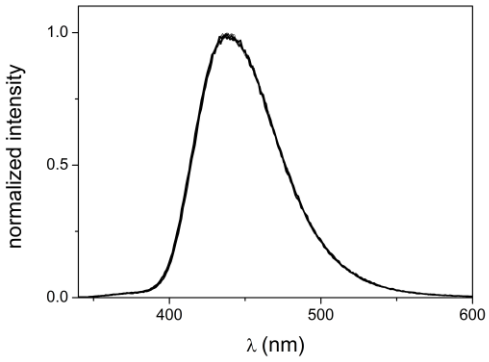

Figure S9. Effect of Ba^{2+} concentration (1.3×10^{-6} to 2.6×10^{-5} mol L^{-1}) on the fluorescence emission profile of **1** in CH_3CN/H_2O (95/5, v/v).

Table S1. Molecular electrostatic potential map charges obtained through computational simulation for probes **1** and **2**

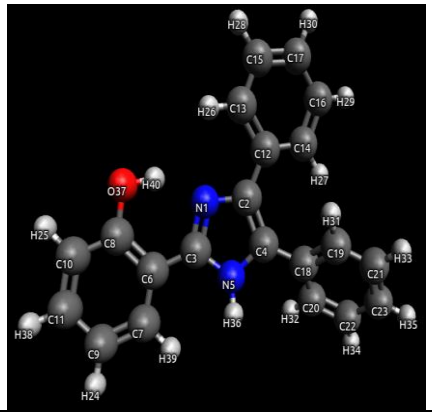

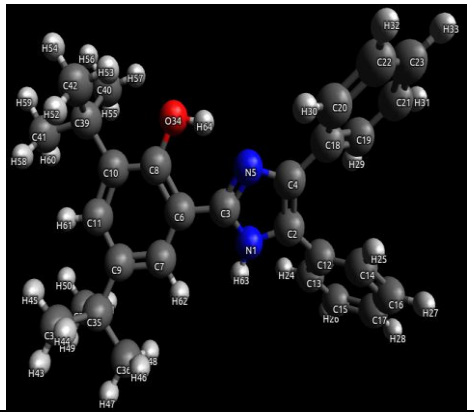

	1			**2**	
Number	Atom	Charge	Number	Atom	Charge
1	**N**	**–0.529195**	1	N	–0.475304
2	C	0.176531	2	C	0.062890
3	C	0.465960	3	C	0.521581
4	C	0.005154	4	C	0.103866
5	N	–0.397905	**5**	**N**	**–0.512104**
6	C	–0.185771	6	C	–0.172940
7	C	–0.109137	7	C	–0.167874
8	C	0.400336	8	C	0.266302
9	C	–0.123126	9	C	0.000580
0	C	–0.191241	10	C	–0.117036
1	C	–0.047079	11	C	–0.202213
2	C	0.089210	12	C	0.152748
3	C	–0.136105	13	C	–0.167904
4	C	–0.074369	14	C	–0.060551
5	C	–0.070818	15	C	–0.062907
6	C	–0.080410	16	C	–0.073318
7	C	–0.080586	17	C	–0.104096
8	C	0.125860	18	C	0.155412
9	C	–0.044899	19	C	–0.081156
0	C	–0.148760	20	C	–0.121623
1	C	–0.059732	21	C	–0.082011
2	C	–0.059302	22	C	–0.071742
3	C	–0.101755	23	C	–0.095143
4	H	0.076873	24	H	0.099443
5	H	0.116977	25	H	0.014796
6	H	0.115200	26	H	0.084348
7	H	0.034571	27	H	0.088607
8	H	0.074224	28	H	0.084952
9	H	0.075657	29	H	0.027107
0	H	0.073157	30	H	0.085871
1	H	0.022952	31	H	0.081755
2	H	0.095694	32	H	0.079476
3	H	0.080920	33	H	0.076346
4	H	0.078863	**34**	**O**	**–0.439655**

Table S1. Molecular electrostatic potential map charges obtained through computational simulation for probes **1** and **2** (cont.)

1			**2**		
Number	Atom	Charge	Number	Atom	Charge
5	H	0.083644	35	C	0.404983
6	H	0.288805	36	C	–0.202886
7	**O**	**–0.564251**	37	C	–0.252938
8	H	0.074675	38	C	–0.159471
9	H	0.093715	39	C	0.497443
0	H	0.355465	40	C	–0.164468
			41	C	–0.287295
			42	C	–0.136008
			43	H	0.029973
			44	H	0.011952
			45	H	0.019568
			46	H	0.026246
			47	H	0.038999
			48	H	0.035237
			49	H	0.059290
			50	H	0.040480
			51	H	0.026212
			52	H	–0.006843
			53	H	0.020274
			54	H	0.012445
			55	H	–0.004325
			56	H	0.027878
			57	H	0.020068
			58	H	0.053397
			59	H	0.050248
			60	H	0.047462
			61	H	0.130654
			62	H	0.084822
			63	H	0.310155
			64	H	0.287944